

# Implications of imaginary chemical potential for model building of QCD

Kouji Kashiwa<sup>1,\*</sup>

<sup>1</sup>*Yukawa Institute for Theoretical Physics, Kyoto University, Kyoto 606-8502, Japan*

Properties of QCD at finite imaginary chemical potential are revisited to utilize for the model building of QCD in low energy regimes. For example, the electric holonomy which is closely related to the Polyakov-loop drastically affects thermodynamic quantities beside the Roberge-Weiss transition line. To incorporate several properties at finite imaginary chemical potential, it is important to introduce the holonomy effects to the coupling constant of effective models. This extension is possible by considering the entanglement vertex. We show justifications of the entanglement vertex based on the derivation of the effective four-fermi interaction in the Nambu–Jona-Lasinio model and present its general form with the local approximation. To discuss how to remove model ambiguities in the entanglement vertex, we calculate the chiral condensate with different  $\mathbb{Z}_3$  sectors and the dual quark condensate.

PACS numbers: 11.30.Rd, 21.65.Qr, 25.75.Nq

## I. INTRODUCTION

Understanding non-perturbative properties of Quantum Chromodynamics (QCD) is one of the important and interesting subjects in nuclear and elementary particle physics. The lattice QCD simulation is a promising method to understand such non-perturbative properties, but the sign problem obscures it at finite real chemical potential ( $\mu_R$ ). Therefore, low energy effective models of QCD are widely used to investigate the QCD phase structure at finite  $\mu_R$ .

In the modeling of QCD in low energy regimes, the chiral condensate and the Polyakov-loop play an important role to describe the chiral and confinement-deconfinement transitions. The famous effective model is the Polyakov-loop extended Nambu–Jona-Lasinio (PNJL) model [1]. In the PNJL model, the quark and gluon contributions are taken into account through the one-loop level effective potential in usual. There is the uncertainty how to introduce the gauge boson contribution. Usually, the chiral part is described by using the Nambu–Jona-Lasinio (NJL) model or similar quark models in effective models. However, the gluon part is less clear than the quark part. There are several effective models for the gluon contribution; for example, the logarithmic potential based on the strong coupling expansion [1, 2], the Ginzburg-Landau type potential [3, 4], the Meisinger-Miller-Ogilvie model [5], the matrix model for the confinement-deconfinement transition [6, 7], the effective potential from the Landau-gauge gluon and ghost propagators [8], the holonomy potential [9] and so on.

In addition to individual parts of the quark and gluon contributions, it is important how to control the strength of the correlation between the quark and gluon contributions in effective models. Importance of such correlation can be clearly seen in the lattice QCD data at finite temperature ( $T$ ) and the imaginary chemical po-

tential ( $\mu_I$ ) [10, 11]. At finite  $\mu_I$ , there is the first-order transition line which is so called the Roberge-Weiss (RW) transition and its endpoint which is so called the RW endpoint [12]. In Ref. [10, 11], the pion mass ( $m_\pi$ ) dependence of the RW endpoint has been predicted by the lattice QCD simulation. At sufficiently large  $m_\pi$ , the order of the RW endpoint is the first-order which is induced by the first-order  $\mathbb{Z}_3$  transition. The first-order RW endpoint becomes the crossover by the explicit breaking of the  $\mathbb{Z}_3$  symmetry at moderate  $m_\pi$ . However, there is the mysterious behavior of the RW endpoint at small  $m_\pi$ ; the order of the transition turns into the first-order! This behavior cannot be reproduced by using simple effective model of QCD, but it can be possible by considering the extension of the coupling constant.

Recently, it has been proposed in Ref. [13, 14] that the confinement-deconfinement transition can be described by using the analogy of the topological order [15] motivated by the recent progress done in Ref. [16] at  $T = 0$  QCD. In the conjecture [13, 14], the nontrivial free-energy degeneracy at finite  $\mu_I$  plays a crucial role. The non-trivial degeneracy is related with the drastic change of the holonomy beside  $\theta = (2k - 1)k/N_c$  in the deconfinement phase where  $\theta$  is the dimensionless chemical potential  $\theta \equiv \mu_I/T$ ,  $N_c$  means the number of color and  $k$  is any integer. Then, we can define the quantum order-parameter which is so called the quark number holonomy on the manifold in all possible boundary condition space which is equivalence to the  $\theta$  space because the boundary condition and the imaginary chemical potential have direct relation, see Ref. [12, 17] as an example. From these viewpoints, holonomy effects in the effective model is crucial not only incorporating the confinement-deconfinement transition into the model, but also understanding the confinement-deconfinement transition itself.

In this paper, we revisit the imaginary chemical potential region to obtain some constraints for the model building of QCD in the low energy regime. This paper is organized as follows. In the next section, we summarize the RW transition and some related topics on it at finite  $\mu_I$ . Section III explains the extension of the effective

---

\* [kouji.kashiwa@yukawa.kyoto-u.ac.jp](mailto:kouji.kashiwa@yukawa.kyoto-u.ac.jp)

model based on Ref. [18]. Then, we show justifications of the extension based on the derivation of the effective four-fermi interaction. In Sec. IV, we calculate the chiral condensate with different  $\mathbb{Z}_3$  sectors to discuss how to remove ambiguities of model parameters. Section V is devoted to summary.

## II. IMAGINARY CHEMICAL POTENTIAL

It is well known that there is a special periodicity in the QCD partition function ( $Z$ ) as a function of  $\theta$ ;

$$Z(\theta) = Z\left(\theta + \frac{2\pi k}{N_c}\right). \quad (1)$$

This means that several quantities have the  $2\pi/N_c$  periodicity. This periodicity is so called the Roberge-Weiss (RW) periodicity.

In the low and high  $T$  region, origins of the RW periodicity is quite different. At low  $T$ , the RW periodicity is realized by only one global minimum on the complex Polyakov-loop ( $\Phi$ ) plane, but does not at high  $T$ . The  $\mathbb{Z}_{N_c}$  images should be needed to realize the RW periodicity at high  $T$ ; for example, the  $\mathbb{Z}_3$  images are  $e^{i2\pi/3}$  and  $e^{i4\pi/3}$  for  $\Phi = 1$ . This difference of origins seems to be related with the confinement and the deconfinement nature. From the different realization of the RW periodicity at low and high  $T$ , there should be the first-order transition and its endpoint at  $\theta = (2k-1)\pi/N_c$ . Those are called the RW transition and the RW endpoint, respectively.

When we change  $\theta$  with fixing  $T$  in the confined phase, the phase of the Polyakov-loop  $\phi$  which is determined from

$$\Phi = \frac{1}{N_c} \text{tr} \mathcal{P} \left[ \exp \left( i \oint_0^\beta A_4(\tau, \vec{x}) d\tau \right) \right] = |\Phi| e^{i\phi}, \quad (2)$$

is continuously rotated as the soliton solution which may be described by the Jacobi elliptic function where  $\mathcal{P}$  means the path ordering operator,  $g$  is the gauge coupling constant and  $\beta$  means the inverse temperature ( $1/T$ ). On the other hand, the Polyakov-loop phase is discontinuously rotated in the deconfined phase. The discontinuous point appears when we across the RW transition line. The electric holonomy ( $\nu$ ) is then discontinuously changed beside the RW transition line and then we obtain

$$d\nu = \lim_{\epsilon \rightarrow 0} \left[ \nu(\theta_{\text{RW}} - \epsilon) - \nu(\theta_{\text{RW}} + \epsilon) \right] \begin{cases} 0 & T < T_{\text{RW}} \\ \frac{2\pi}{N_c} & T > T_{\text{RW}}, \end{cases}$$

where we define  $d\nu$  as  $\{d\nu \mid 0 \leq d\nu \leq 2\pi\}$ . Just on the RW endpoint,  $d\nu$  depends on its order: If the RW endpoint is first-order,  $d\nu$  should be  $2\pi/N_c$ . Because of this behavior,  $\theta$ -even quantities such as the entropy density

and pressure should have the cusp, but  $\theta$ -odd quantities such as the quark number density have the gap at  $\theta = (2k-1)\pi/N_c$  above the RW endpoint.

The RW transition and endpoint have interesting phenomena as discussed above, but it may have more mysterious behavior which is the triple-point realization of the RW endpoint at small  $m_\pi$  which is predicted by the lattice QCD simulation [10, 11]. At sufficiently large  $m_\pi$ , the order of the RW endpoint is the first-order. This first-order RW endpoint becomes the crossover by the explicit breaking of the  $\mathbb{Z}_3$  symmetry when we set  $m_\pi$  as moderate values. However, the order of the RW transition turns into the first-order again at small  $m_\pi$ . This behavior is considered as the consequence of the correlation between the chiral and the confinement-deconfinement transition nature, but it is still under debate. By using simple effective models such as the standard PNJL model, this behavior cannot be reproduced; for example, see Ref. [19]. To resolve this point, we need extension of the effective model. Actually, by extending the coupling constant in the PNJL model, we can reproduce the lattice QCD simulation [18], but the exact form of the extended coupling constant is not discussed so far. In the next section, we revisit this point.

## III. ENTANGLEMENT VERTEX

In this study, we use the PNJL model. The simplest two-flavor and three-color PNJL model Lagrangian density becomes

$$\mathcal{L} = \bar{q}(i\not{D} - m_0)q + G[(\bar{q}q)^2 + (\bar{q}i\gamma_5\vec{\tau}q)^2] - \beta V \mathcal{U}, \quad (3)$$

where  $D^\mu = \partial^\mu + i\delta_0^{\nu a} A^{\nu a} \lambda_a/2$  with Gell-Mann matrices  $\lambda_a$ ,  $m_0$  expresses the current quark mass,  $G$  is the coupling constant and  $V$  does the three-dimensional volume. The term  $\mathcal{U}$  expresses the gluon contribution. Model parameters in the NJL part such as  $m_0$ ,  $G$  and the cutoff of the three-dimensional momentum integration ( $\Lambda$ ) is determined by using the  $m_\pi$  and pion decay constant. The actual values used in this study are  $m_0 = 5.5$  MeV,  $G = 5.498$  GeV $^{-2}$ ,  $\Lambda = 613.5$  MeV.

In this study, we use the mean-field approximation; see Ref. [18] for the details of the calculation. The actual thermodynamic potential can be obtained from the Lagrangian density (3) as

$$\Omega = -4 \int \frac{d^3p}{(2\pi)^3} \left[ 3E(p) + T(\ln f^- + \ln f^+) \right] + 2G\sigma^2 + \mathcal{U}, \quad (4)$$

where

$$\begin{aligned} f^- &= 1 + 3(\Phi + \bar{\Phi}e^{-\beta E^-(p)})e^{-\beta E^-(p)} + e^{-3\beta E^-(p)}, \\ f^+ &= 1 + 3(\bar{\Phi} + \Phi e^{-\beta E^+(p)})e^{-\beta E^+(p)} + e^{-3\beta E^+(p)}, \end{aligned} \quad (5)$$

here  $\bar{\Phi}$  is the conjugate of  $\Phi$  and  $E^\mp(p) = E(p) \mp \mu =$

$\sqrt{p^2 + M^2} \mp \mu$  with  $M = m_0 - 2G\sigma$  and the chemical potential  $\mu = (\mu_R, \mu_I)$ . The quantity  $\sigma$  becomes the chiral condensate in the present model. The gluon contribution  $\mathcal{U}$  is taken into account via the logarithmic Polyakov-loop effective potential [2] as

$$\frac{\mathcal{U}}{T^4} = -\frac{1}{2}b_2(T)\bar{\Phi}\Phi + b_4(T)\ln\left[1 - 6\bar{\Phi}\Phi + 4(\bar{\Phi}^3 + \Phi^3) - 3(\bar{\Phi}\Phi)^2\right], \quad (6)$$

where

$$b_2(T) = a_0 + a_1\left(\frac{T_0}{T}\right) + a_2\left(\frac{T_0}{T}\right)^2 + a_3\left(\frac{T_0}{T}\right)^3, \\ b_4(T) = b_4\left(\frac{T_0}{T}\right)^3, \quad (7)$$

with  $a_0 = 3.51$ ,  $a_1 = -2.56$ ,  $a_2 = 15.2$ ,  $a_3 = -0.62$  and  $b_4 = -1.68$ . These parameters are determined to reproduce the lattice QCD data such as the energy and the entropy density in the pure gauge limit. The parameter  $T_0$  controls the confinement-deconfinement temperature ( $T_D$ ) in the pure gauge limit and thus we set  $T_0 = 270$  MeV because we are interested in the quenched calculation.

In Ref. [18], the extension of the PNJL model coupling constant has been proposed. The extension has been done by the replacement

$$G \rightarrow G(\Phi) = G[1 - \alpha_1\bar{\Phi}\Phi - \alpha_2(\bar{\Phi}^3 + \Phi^3)], \quad (8)$$

where  $\alpha_1$  and  $\alpha_2$  are new parameters. This extended coupling constant is so called the entanglement vertex. In the extension, the  $\mathbb{Z}_3$  symmetry of the vertex is assumed. This interaction strongly correlates the chiral and the confinement-deconfinement transition. The entanglement nature is deeply related with the nonlocal properties of the interaction which is usually hidden in the local PNJL model.

From the derivation of the NJL and also the PNJL model, the nonlocal nature is a natural consequence. The PNJL model can be obtained starting from QCD partition function by using the color-current expansion and some *ansatz* for gluon properties; details of the nonlocal PNJL model, for example, see Ref. [20–22] and references therein. The nonlocal interaction should feel effects coming from the gluon two-point function since the interaction forms

$$\mathcal{L}_{\text{int}}(x) = g^2 j_\mu^a(x) \int d^4y W_{\mu\nu}^{(2)ab} j_\nu^b(y), \quad (9)$$

where  $j_\mu^a = \bar{q} \frac{\lambda^a}{2} \gamma_\mu q$  is the color-current,  $W^{(2)}$  is the gluon two-point function without quark loops because we use the color-current expansion around  $j = 0$ . Since the two-point function does not have quark loops,  $W^{(2)}$  should be  $\mathbb{Z}_{N_c}$  symmetric form. To obtain the local version of the PNJL model, we should replace the two-point function as the delta function since we assume  $W^{(2)}$  is very short

range. The gluon follows the adjoint representation of  $SU(N_c)$ , and thus the entanglement vertex should obey the adjoint representation nature.

To introduce the adjoint representation nature to the entanglement vertex, we refer to the structure of the gluon one-loop effective potential and the Bose distribution function with the electric holonomy. Those manifest the  $\mathbb{Z}_3$  symmetric form and other adjoint representation natures. So, more general form of the entanglement vertex for the color singlet sector can be written as

$$G(\Phi) = G_N \left[ 1 + \left( \sum_{n=1}^8 \alpha'_n C_n e^{-n\beta E} \right)^\gamma \right], \quad (10)$$

where  $G_N$ ,  $\alpha'_n$  and  $\gamma$  are parameters,  $E = |\vec{p}|$  is the typical energy scale in the momentum space and

$$C_1 = C_7 = 1 - 9\bar{\Phi}\Phi, \\ C_2 = C_6 = 1 - 27\bar{\Phi}\Phi + 27(\bar{\Phi}^3 + \Phi^3), \\ C_3 = C_5 = -2 + 27\bar{\Phi}\Phi - 81(\bar{\Phi}\Phi)^2, \\ C_4 = 2 \left[ -1 + 9\bar{\Phi}\Phi - 27(\bar{\Phi}^3 + \Phi^3) + 81(\bar{\Phi}\Phi)^2 \right], \\ C_8 = 1. \quad (11)$$

For details of functions  $C_n$ , see Ref. [23]. Even if we assume the effective gluon mass such as the Gribov-Stingl form at finite  $T$  as

$$D_T^{(T,L)} \propto \frac{d_{t,l}(p^2 + d_{t,l}^{-1})}{(p^2 + r_{t,l}^2)^2}, \quad (12)$$

we then obtain same expression of  $C_n$  [8], where  $D_T^T$  ( $D_T^L$ ) are the tree-dimensional transverse (longitudinal) gluon propagator. Thus, we can expect that above expression is general form for the entanglement vertex.

When we assume that the  $W^{(2)}$  is short range, higher-order terms of  $e^{-\beta E}$  in Eq. (10) should be suppressed and then only  $C_1$  is relevant. From here, we set  $\gamma = 1$  to make our discussion simple and it is not an essential point in the level of present discussions. Thus, we can effectively rewrite the coupling constant (10) as the simple form

$$G(\Phi) \sim G_N \left( 1 + \alpha \bar{\Phi}\Phi \right), \quad (13)$$

where  $G_N$  is corresponding to  $G$  in the original PNJL model in this case because  $\bar{\Phi}$  and  $\Phi$  do not affect the physics at  $T = 0$ . This form is similar to Eq. (8), but it is more general. If we set  $\alpha = -\alpha_1$  and  $\alpha_2 = 0$  with  $\gamma = 1$ , this vertex is perfectly matched with the vertex (8). From present representation, terms proportional to  $(\bar{\Phi}^3 + \Phi^3)$  becomes the higher-order contribution and thus it can be safely neglected in the level discussed here. In the effective model construction, important operation is the parameter fixing. Details of parameter fixing are discussed in the next section.

Recently, it has been numerically shown that the  $\mathbb{Z}_3$

factor can affect the Landau-gauge gluon propagator in the deconfined phase by using the pure gauge calculation in Ref. [24]. In the gluon propagator, the  $\mathbb{Z}_3$  factors can appear via  $\mathcal{A}_4^{ab} = \mathcal{A}_4^a - \mathcal{A}_4^b$  when we consider the background gauge field where  $\mathcal{A}_4$  is the temporal component of the field and  $a, b$  run  $1, \dots, N_c$  because the gluon obeys the adjoint representation. For  $a = b$  diagonal sectors, the  $\mathbb{Z}_{N_c}$  factor cannot appear because of the exact cancellation of the  $\mathbb{Z}_3$  factors. On the other hand, the non-diagonal  $a \neq b$  sectors may feel the effect via the effective gluon mass. Also, in the confined and deconfined phases, the elementary degree of freedom is drastically different; it is glueball in the confined phase, but it is gluon in the deconfined phase. Both reasons may lead to the lattice QCD predicted phenomena, but we need more careful investigation for the lattice QCD data to conclude it. In the short range limit of  $W^{(2)}$ , the color structure is extremely simplified and thus above effect cannot appear in the local PNJL model. To incorporate the effects, we should consider the nonlocal PNJL model, but it seems a difficult task. Even in the modern nonlocal PNJL model [2, 22, 25–28], we implicitly use the simplification of the color structure of the four-fermi interaction. At present, we do not know how important this effects for the gauge invariant observable, and thus we assume that  $W^{(2)}$  is short range to neglect the effect as a first step. This problem will be discussed in the nonlocal PNJL model elsewhere.

#### IV. NUMERICAL RESULTS

In this section, we discuss how to remove ambiguities of the parameters in the entanglement vertex by using lattice QCD simulations with the quenched approximation. The entanglement vertex correlates the chiral and the confinement-deconfinement transition and thus the chiral condensate with different  $\mathbb{Z}_3$  sectors seems to be a promising quantity to remove ambiguities of model parameters. The existence of non-trivial  $\mathbb{Z}_3$  sectors which is characterized by  $\phi = \frac{2\pi}{3}$  and  $\frac{4\pi}{3}$  is not trivial in the system with dynamical quarks. Therefore, we here consider the quenched approximation since all possible  $\mathbb{Z}_3$  sectors are well defined. The calculation of the chiral condensate with the different  $\mathbb{Z}_3$  sector was done in Ref. [29, 30] and thus we follow their calculation by using present extended model. In the calculation [30], they introduce the  $T$ -dependent coupling constant by hand, but this effect is automatically introduced in the present entanglement PNJL model.

In this study, we first calculate  $\Phi$  in the pure gauge limit to consider the quenched calculation. The Polyakov-loop with non-trivial  $\mathbb{Z}_3$  sectors,  $\Phi_{\frac{2\pi}{3}}$  and  $\Phi_{\frac{4\pi}{3}}$ , are obtained by the  $\mathbb{Z}_3$  transformation from the Polyakov-loop with the trivial  $\mathbb{Z}_3$  sector,  $\Phi_0$ . Figure 1 shows  $\Phi$  with  $\phi = 0$  and  $\phi = \frac{2\pi}{3}$  in the pure gauge limit as a function of  $T$ . After this calculation, we substitute those  $\Phi$  to the PNJL model and then we minimize the

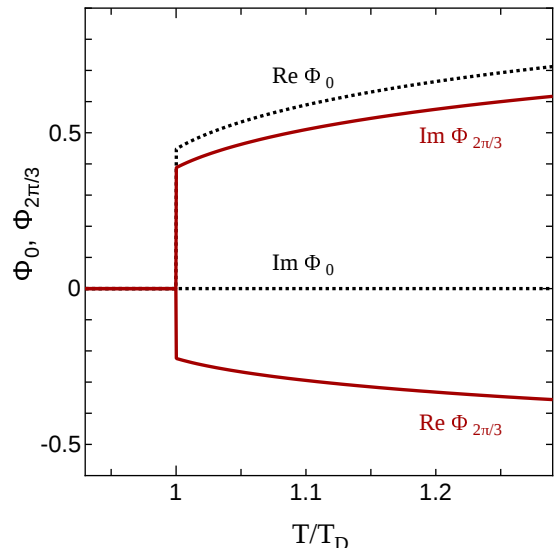


FIG. 1. The  $T$ -dependence of  $\Phi$  with different  $\mathbb{Z}_3$  sectors in the pure gauge limit. The dotted and solid lines represent the result with  $\phi = 0$  and  $\phi = \frac{2\pi}{3}$ , respectively.

thermodynamic potential as a function of  $\sigma$ . This procedure is corresponding to the quenched calculation of the PNJL model.

Figure. 2 shows the chiral condensate with different  $\mathbb{Z}_3$  sectors at  $\mu = 0$  as a function of  $T$ . The top and bottom panels of Fig. 2 show  $\sigma/\sigma_0$  with the trivial  $\mathbb{Z}_3$  sector  $\phi = 0$  and that with  $\phi = 2\pi/3$  where  $\sigma_0$  is  $\sigma$  at  $T = \mu = 0$ , respectively. It is natural to assume that the entanglement vertex is decreased with increasing  $T$  and thus the sign of  $\alpha$  is negative because of properties of the running coupling in QCD. When  $\alpha$  is small in the bottom panel, the chiral condensate increases above  $T_D$ , but it decreases in the large- $\alpha$  case. There is the drastic change in the  $T$ -dependence of  $\sigma$  and thus we can determine the parameters in the entanglement vertex by using precise quenched lattice QCD data. At least in Ref. [29, 30], the chiral condensate with nontrivial  $\mathbb{Z}_3$  sectors are decreased and thus  $\alpha$  should be considerably large. To conclude the detailed value of  $\alpha$ , we need more precise quenched lattice QCD data.

Other promising quantity to remove the model ambiguities is the dual quark condensate [31–33]. The dual quark condensate is the order-parameter of the  $\mathbb{Z}_{N_c}$  symmetry breaking as same as the Polyakov-loop. This quantity has been calculated by using the lattice QCD simulation [31–33], the Schwinger-Dyson equations [34], the effective model of QCD [35], the functional renormalization group equations [36] and so on. The dual quark condensate is defined as

$$\Sigma_\sigma^{(n)} = - \int \frac{d\varphi}{2\pi} e^{-in\varphi} \sigma_\varphi, \quad (14)$$

where  $\varphi$  specifies the boundary condition of the tempo-

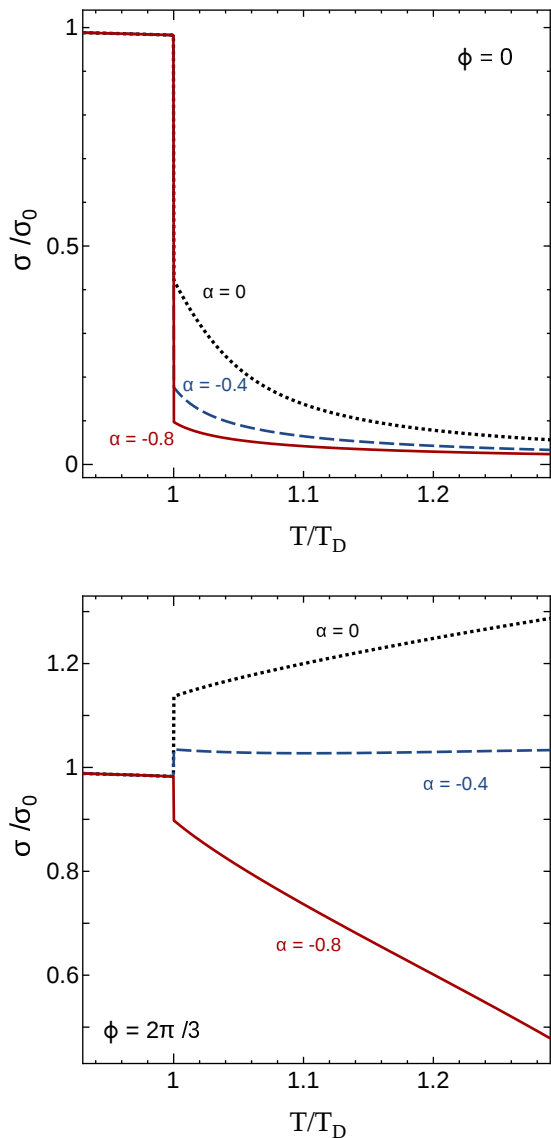


FIG. 2. The  $T$ -dependence of the chiral condensate with different  $\mathbb{Z}_3$  sectors normalized by own value at  $T = \mu = 0$ . The top and bottom panels show  $\sigma$  with  $\phi = 0$  and that  $\phi = 2\pi/3$ , respectively. The dotted, dashed and solid lines represent the result with  $\alpha = 0, -0.4$  and  $-0.8$ , respectively.

ral direction for quarks,  $n$  means the winding number for the temporal direction and  $\sigma$  is the  $\varphi$ -dependent chiral condensate. Usually, we take  $n = 1$ . The boundary condition and the imaginary chemical potential have direct relation,  $\theta = \varphi - \pi$ . In the system with dynamical quarks, there are some problems in the dual quark condensate [37–39], but we can expect that the quenched calculations where the dual quark condensate is well defined can provide the important information for the effective model construction. At present, quenched lattice QCD data for the dual quark condensate are limited and thus we do not quantitatively compare our results with the

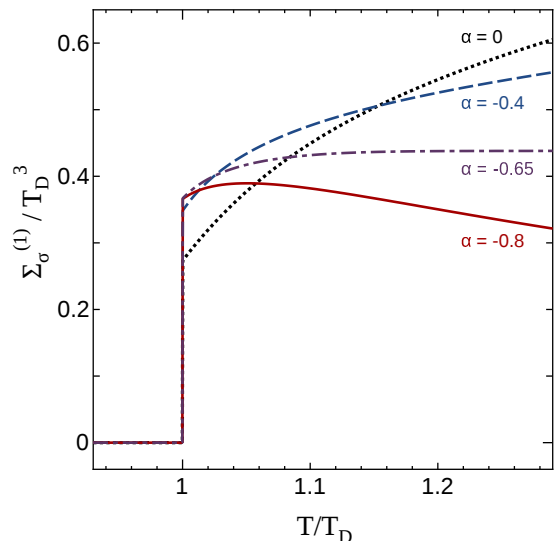


FIG. 3. The  $T$ -dependence of  $\Sigma_\sigma^{(1)}$  at  $\mu_R = 0$ . The dotted, dashed, dot-dashed and solid lines represent the result with  $\alpha = 0, -0.4, -0.65$  and  $-0.8$ , respectively.

lattice data. Figure 3 shows the  $T$ -dependence of  $\Sigma_\sigma^{(1)}$  at  $\mu = 0$  with different values of  $\alpha$ . We can find the visible  $\alpha$ -dependence in  $\Sigma_\sigma^{(1)}$ . At least in quenched lattice QCD data we can access [31],  $\Sigma_\sigma^{(1)}$  increases with increasing  $T$  and thus extremely strong  $\alpha$  may be excluded, but we need more quenched lattice QCD data to conclude it. The critical value ( $\alpha_c$ ) which leads to the flat behavior of  $\Sigma_\sigma^{(1)}$  above  $T_D$  exists in the range  $-0.7 < \alpha_c < -0.6$ .

Finally, we propose a new quantity which can describe the confinement-deconfinement transition based on the dual quark condensate. The quantity is defined as

$$\Sigma_{\mathcal{O}}^{(n)} = \int \frac{d\varphi}{2\pi} e^{-in\varphi} \mathcal{O}(\varphi), \quad (15)$$

where  $\mathcal{O}$  is the  $\theta$ -even quantity. If we consider that the dual quark condensate measures how information of  $\mathbb{Z}_3$  images are missed in the calculation of Eq. (14) when the gauge configuration is fixed to the trivial  $\mathbb{Z}_3$  sector, there is no need to use  $\sigma$  as the integrand of Eq. (14). It is related with the study based on the nontrivial free energy degeneracy in Ref. [13, 14]. Figure 4 shows  $T$ -dependence of the quantity (15) with  $\mathcal{O} = P$  and  $n = 1$  where  $P$  is the pressure. We can see that this quantity also describes the confinement-deconfinement transition. This behavior is, of course, trivial from the viewpoint of the RW periodicity. It is interesting to calculate it in the system with dynamical quarks and some theories where we cannot easily calculate the chiral condensate.



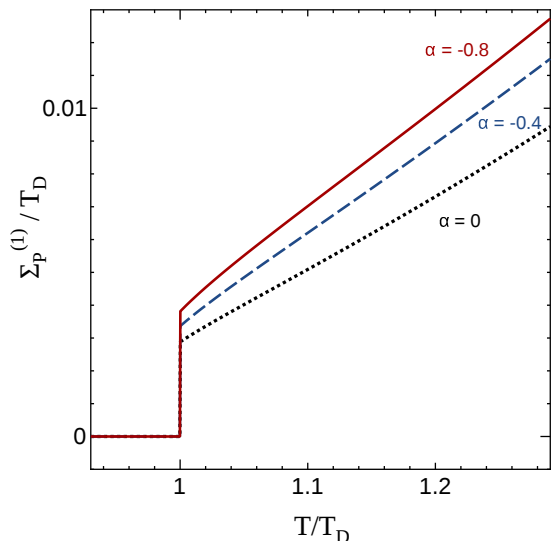


FIG. 4. The  $T$ -dependence of  $\Sigma_P^{(1)}$ . The dotted, dashed and solid lines represent the result with  $\alpha = 0, -0.4$  and  $-0.8$ , respectively.

## V. SUMMARY

In this paper, we have discussed the extension of the effective model such as the Polyakov-loop extended Nambu–Jona-Lasinio model. Firstly, implications of QCD properties in the imaginary chemical potential region to the effective model construction has been discussed. Then the importance of the entanglement vertex [18] has been explained from the derivation of the effective four-fermi interaction from QCD partition function with some approximations and *ansatz*.

Secondly, we have shown that the general form of the entanglement vertex which should be needed to reproduce the lattice QCD prediction at finite  $\mu_1$  [10, 11]. The general form is refer to the structure of the gluon one-loop effective potential and the Bose distribution function and then it naturally leads to the  $\mathbb{Z}_3$  symmetric form.

Finally, the chiral condensate with different  $\mathbb{Z}_3$  sectors and the dual quark condensate with  $n = 1$  have been calculated by using the PNJL model with the entanglement vertex. The entanglement vertex has one parameter  $\alpha$  when we assume  $\gamma = 1$  at least in the next leading-order of  $e^{-\beta E}$ . When  $\alpha$  is small, the chiral condensate with the non-trivial  $\mathbb{Z}_3$  sector increases even above  $T_D$ , but it decreases in the large- $\alpha$  case. This result suggests that we can well remove the ambiguity of the parameters by using the  $T$ -dependence of the chiral condensate with the different  $\mathbb{Z}_3$  sectors. Also, we can find visible  $\alpha$ -dependence in the dual quark condensate and thus this quantity should be the promising quantity to remove the ambiguity of the parameters. From qualitative behavior of quenched lattice QCD data [29–31], we may exclude extremely strong and weak  $\alpha$  values, but we need more quenched lattice QCD data to conclude it. In addition to above results, we propose new quantity which can describe the confinement-deconfinement transition based on the dual quark condensate.

## ACKNOWLEDGMENTS

K.K. thanks A. Ohnishi and H. Kouno for useful comments. K.K. is supported by Grants-in-Aid for Japan Society for the Promotion of Science (JSPS) fellows No.26-1717.

- 
- [1] K. Fukushima, *Phys.Lett.* **B591**, 277 (2004), [arXiv:hep-ph/0310121 \[hep-ph\]](#).
  - [2] T. Hell, S. Rossner, M. Cristoforetti, and W. Weise, *Phys. Rev.* **D81**, 074034 (2010), [arXiv:0911.3510 \[hep-ph\]](#).
  - [3] C. Ratti, M. A. Thaler, and W. Weise, *Phys.Rev.* **D73**, 014019 (2006), [arXiv:hep-ph/0506234 \[hep-ph\]](#).
  - [4] S. Roessner, C. Ratti, and W. Weise, *Phys.Rev.* **D75**, 034007 (2007), [arXiv:hep-ph/0609281 \[hep-ph\]](#).
  - [5] P. N. Meisinger, T. R. Miller, and M. C. Ogilvie, *Phys.Rev.* **D65**, 034009 (2002), [arXiv:hep-ph/0108009 \[hep-ph\]](#).
  - [6] A. Dumitru, Y. Guo, Y. Hidaka, C. P. K. Altes, and R. D. Pisarski, *Phys.Rev.* **D83**, 034022 (2011), [arXiv:1011.3820 \[hep-ph\]](#).
  - [7] K. Kashiwa, R. D. Pisarski, and V. V. Skokov, *Phys.Rev.* **D85**, 114029 (2012), [arXiv:1205.0545 \[hep-ph\]](#).
  - [8] K. Fukushima and K. Kashiwa, *Phys.Lett.* **B723**, 360 (2013), [arXiv:1206.0685 \[hep-ph\]](#).
  - [9] E. Shuryak and T. Sulejmanpasic, *Phys. Lett.* **B726**, 257 (2013), [arXiv:1305.0796 \[hep-ph\]](#).
  - [10] M. D’Elia and F. Sanfilippo, *Phys. Rev.* **D80**, 111501 (2009), [arXiv:0909.0254 \[hep-lat\]](#).
  - [11] C. Bonati, G. Cossu, M. D’Elia, and F. Sanfilippo, *Phys.Rev.* **D83**, 054505 (2011), [arXiv:1011.4515 \[hep-lat\]](#).
  - [12] A. Roberge and N. Weiss, *Nucl.Phys.* **B275**, 734 (1986).
  - [13] K. Kashiwa and A. Ohnishi, *Phys. Lett.* **B750**, 282 (2015), [arXiv:1505.06799 \[hep-ph\]](#).
  - [14] K. Kashiwa and A. Ohnishi, (2016), [arXiv:1602.06037 \[hep-ph\]](#).
  - [15] X. Wen, *Int.J.Mod.Phys.* **B4**, 239 (1990).
  - [16] M. Sato, *Phys.Rev.* **D77**, 045013 (2008), [arXiv:0705.2476 \[hep-th\]](#).
  - [17] K. Kashiwa and T. Misumi, *JHEP* **1305**, 042 (2013), [arXiv:1302.2196 \[hep-ph\]](#).
  - [18] Y. Sakai, T. Sasaki, H. Kouno, and M. Yahiro, *Phys. Rev.* **D82**, 076003 (2010), [arXiv:1006.3648 \[hep-ph\]](#).
  - [19] T. Sasaki, Y. Sakai, H. Kouno, and M. Yahiro, *Phys. Rev.* **D84**, 091901 (2011), [arXiv:1105.3959 \[hep-ph\]](#).
  - [20] B. Van den Bossche, in *Research Workshop on Deconfinement at Finite Temperature and Density Dubna, Russia*,

- October 1-25, 1997 (1997) [arXiv:nucl-th/9807010](#) [nucl-th].
- [21] K.-I. Kondo, *Phys.Rev.* **D82**, 065024 (2010), [arXiv:1005.0314](#) [hep-th].
- [22] K. Kashiwa, T. Hell, and W. Weise, *Phys.Rev.* **D84**, 056010 (2011), [arXiv:1106.5025](#) [hep-ph].
- [23] C. Sasaki and K. Redlich, *Phys.Rev.* **D86**, 014007 (2012), [arXiv:1204.4330](#) [hep-ph].
- [24] P. J. Silva and O. Oliveira, (2016), [arXiv:1601.01594](#) [hep-lat].
- [25] T. Hell, S. Roessner, M. Cristoforetti, and W. Weise, *Phys.Rev.* **D79**, 014022 (2009), [arXiv:0810.1099](#) [hep-ph].
- [26] A. E. Radzhabov, D. Blaschke, M. Buballa, and M. K. Volkov, *Phys. Rev.* **D83**, 116004 (2011), [arXiv:1012.0664](#) [hep-ph].
- [27] V. Pagura, D. Gomez Dumm, and N. N. Scoccola, *Phys. Lett.* **B707**, 76 (2012), [arXiv:1105.1739](#) [hep-ph].
- [28] J. P. Carlomagno, D. Gmez Dumm, and N. N. Scoccola, *Phys. Rev.* **D88**, 074034 (2013), [arXiv:1305.2969](#) [hep-ph].
- [29] S. Chandrasekharan and N. H. Christ, *Lattice '95. Proceedings, International Symposium on Lattice Field Theory, Melbourne, Australia, July 11-15, 1995*, *Nucl. Phys. Proc. Suppl.* **47**, 527 (1996), [arXiv:hep-lat/9509095](#) [hep-lat].
- [30] S. Chandrasekharan and S.-z. Huang, *Phys. Rev.* **D53**, 5100 (1996), [arXiv:hep-ph/9512323](#) [hep-ph].
- [31] E. Bilgici, F. Bruckmann, C. Gattringer, and C. Hagen, *Phys.Rev.* **D77**, 094007 (2008), [arXiv:0801.4051](#) [hep-lat].
- [32] E. Bilgici, F. Bruckmann, J. Danzer, C. Gattringer, C. Hagen, E. M. Ilgenfritz, and A. Maas, *Few Body Syst.* **47**, 125 (2010), [arXiv:0906.3957](#) [hep-lat].
- [33] E. Bilgici, “Signatures of confinement and chiral symmetry breaking in spectral quantities of lattice Dirac operators,” University of Graz, 2009, (<http://physik.uni-graz.at/itp/files/bilgici/dissertation.pdf>).
- [34] C. S. Fischer, *Phys.Rev.Lett.* **103**, 052003 (2009), [arXiv:0904.2700](#) [hep-ph].
- [35] K. Kashiwa, H. Kouno, and M. Yahiro, *Phys.Rev.* **D80**, 117901 (2009), [arXiv:0908.1213](#) [hep-ph].
- [36] J. Braun, L. M. Haas, F. Marhauser, and J. M. Pawłowski, *Phys. Rev. Lett.* **106**, 022002 (2011), [arXiv:0908.0008](#) [hep-ph].
- [37] S. Benič, *Phys.Rev.* **D88**, 077501 (2013), [arXiv:1305.6567](#) [hep-ph].
- [38] F. Marquez, A. Ahmad, M. Buballa, and A. Raya, *Phys. Lett.* **B747**, 529 (2015), [arXiv:1504.06730](#) [nucl-th].
- [39] Z. Zhang and Q. Miao, *Phys. Lett.* **B753**, 670 (2016), [arXiv:1507.07224](#) [hep-ph].